Scientia Iranica B (2021) 28(4), 2133–2149

Sharif University of Technology
Scientia Iranica
Transactions B: Mechanical Engineering
http://scientiairanica.sharif.edu

A study on turbulence-combustion interaction and sub-grid scale model in the simulation of methane pool fire using LES

M. Safarzadeh, G. Heidarinejad, and H. Pasdarshahri*

Faculty of Mechanical Engineering, Tarbiat Modares University, Tehran, P.O. Box 14115-143, Iran.

Received 23 April 2019; received in revised form 22 May 2020; accepted 1 February 2021

KEYWORDS
Pool fire;
Eddy dissipation model;
Infinite fast chemistry;
Smagorinsky SGS;
One-equation SGS;
LES-IQ.

Abstract. In this paper, the effect of the combustion and turbulence Sub-Grid Scale (SGS) model on simulation of a pool fire turbulence field has been studied in open source Cumputational Fluid Dynamic (CFD) software, OpenFOAM. Two combustion models: Eddy Dissipation Model (EDM) and infinite fast chemistry, with the one-equation and Smagorinsky SGS model, are evaluated for a large-scale pool fire. In general, fast kinetic-based combustion models predict excessive heat release rate. The mean squared of the velocity fluctuations is over-predicted. In this simulation, the turbulence models have no significant effect on the results. In fact, the effect of the combustion model is dominant. The EDM combustion model is more compatible when used with the one-equation SGS model and improves the results compared to other cases. In addition, the infinite fast chemistry combustion model is not a suitable model for fire simulation.

1. Introduction

Pool fire is one of the most common fire scenarios that examines the efficiency of different modeling methods in fire dynamic simulations [1–3]. It is a multi-physics phenomenon which deals with combustion kinetics, turbulent flow, heat transfer and soot production [4–6].

In the early modeling of the fire, the Reynolds Averaged Navier Stokes (RANS) methods were used in order to model the turbulent flow in the fire scenarios [7,8]. In 1994, McGrattan [9] developed a Large Eddy Simulation (LES) code for fire simulation in an open and closed (compartment) area. In 2000, Fire Dynamic Simulator (FDS) software was released based on the LES method [10,11].

Combustion models determine the reaction rate in the reacting flow and are essential in a turbulent combustion regime [12,13]. Xue et al. [14] considered the results of three combustion models: Volumetric Heat Source (VHS), Eddy Brake-Up (EBU), and prePDF, for three fire scenarios in large and small rooms, as well as a fire in a tunnel. The results of these three methods were compared using the $k-\varepsilon$ model. The prePDF combustion model was preferred with respect to the others. Huang et al. [15] also considered three combustion models: VHS, EBU, and prePDF with the $k-\varepsilon$ model, for a fire scenario in a room. As reported, the VHS model has the least computational time but is not a suitable model for estimating species because chemical reactions are not considered in this model.

Some other studies have tested the effectiveness of various combustion models for the LES method [16]. Yeoh et al. [17] compared the results of two combustion

*. *Corresponding author. Tel.: 98 21 82883963*
E-mail addresses: m.safarzadeh@modares.ac.ir (M. Safarzadeh); gheidari@modares.ac.ir (G. Heidarinejad); pasdar@modares.ac.ir (H. Pasdarshahri)

doi: 10.24200/sci.2021.53390.3217

models: EBU and laminar flamelet using the LES method, for combustion in one room, two and more rooms. They reported that the results of these two models are almost similar but the computational cost of the laminar flamelet method is lower.

Yang et al. [18] examined the three combustion models: the Eddy Dissipation Concept (EDC), infinite fast chemistry, and a combustion model based on a mixture fraction using FDS software for the fire scenario in a single room with an opening. In this study, the combustion model based on the mixture fraction with two-step kinetics was defined. The results showed that the prediction of the heat release rate in two-step kinetics was more accurate than that of the one-step. Maragkos and Merci [19] compared the efficiency of the Eddy Dissipation Model (EDM) combustion model in OpenFOAM and FDS software. They predicted the mean flame temperature by the OpenFOAM of around 100 Kelvin higher than the experimental results package.

Pasdarshahri et al. [20] examined the simulation of a large pool fire with Smagorinsky and one-equation Sub-Grid Scale (SGS) using the infinite fast chemistry combustion model. It was observed that the model of one-equation and Smagorinsky estimated the mean vertical velocity with 7% and 12% differences from those of the experimental results, respectively, but the computational time of one-equation SGS is about 16% higher than of Smagorinsky.

Yuen et al. [21] studied the three sub-grid models of Smagorinsky, Wale, and Verman using the laminar flamelet model, and concluded that the WALE SGS model was more compatible with the laminar flamelet method. They also presented [22] the appropriate value for three constant coefficients of Smagorinsky, turbulence Prandtl and Schmidt numbers, which are more compatible with the laminar flamelet combustion model. Maragkos et al. [23] corrected EDM model coefficients by comparing EDM and EDC results in a small pool fire. In this study, the EDM combustion coefficient changed from 1 to 8 and concluded that coefficient 1 predicts a more accurate result.

According to this review, the combustion model should be selected according to the fire scenario and the turbulence model [24].

In previous studies, no comparison has been made between different combustion models and SGS methods in the turbulence field of pool fire simulation. The contributions of the present study mainly refer to: Investigation of the turbulence field and comparison of the combustion model and SGS methods in pool fire modeling. So, in the present study, a large scale pool fire was considered, to examine the effect of the combustion and the SGS models. The importance of using a suitable combustion model in modeling a large scale pool fire turbulence field has been investigated. Considering the simple scenario, the efficiency of the EDM and the infinite fast chemistry combustion models in two different models of the Smagorinsky and one-equation SGS are examined, to simulate the turbulence field in the large pool fire.

2. Governing equation

The equations of non-premixed reacting flow such as continuity, momentum, energy, species and turbulence equations can be filtered by using the low-Mach-number Favre-filtering method; in this case, the required equations for the combustion modeling are Eqs. (1)–(4) [25]:

$$\frac{\partial(\bar{\rho})}{\partial t}+\frac{\partial(\bar{\rho}\tilde{u}_i)}{\partial x_i}=0, \tag{1}$$

$$\frac{\partial(\bar{\rho}\tilde{u}_j)}{\partial t}+\frac{\partial(\bar{\rho}\bar{u}_i\tilde{u}_j)}{\partial x_i}= -\frac{\partial\bar{p}}{\partial x_i}+\frac{\partial\bar{\tau}_{ij}}{\partial x_i}-\frac{\partial(\bar{\tau}_{u_iu_j})}{\partial x_i}+(\bar{\rho}-\rho_{ref})g_i, \tag{2}$$

$$\bar{\rho}C_p\frac{\partial(\tilde{T})}{\partial t}+\bar{\rho}C_p\tilde{u}_i\frac{\partial(\tilde{T})}{\partial x_i}= \frac{D\bar{p}}{Dt}-\frac{\partial\bar{q}_i}{\partial x_i}+\frac{\partial\bar{\tau}_{u_iT}}{\partial x_i}+\bar{\omega}_\tau+S_{rad}, \tag{3}$$

$$\frac{\partial(\bar{\rho}\tilde{\varphi})}{\partial t}+\frac{\partial(\bar{\rho}\bar{u}_i\tilde{\varphi})}{\partial x_i}=-\frac{\partial\bar{q}_\varphi}{\partial x_i}+\frac{\partial\bar{\tau}_{u_i\varphi}}{\partial x_i}+S_\varphi. \tag{4}$$

In these equations, ρ is the mixture density, u_i, P and T are the velocity, pressure, and temperature, respectively. φ can be each scalar quantity (such as mass fraction) and ω_T is the rate of heat generation by the combustion. The terms S_{rad} and S_φ are the radiation heat transfer and production term in the equations of energy and scalar quantity. In Eqs. (2) to (4), viscous stress tensor, species diffusion vector, and heat flux vector are modeled using the Newton, Fourier and Fick rules, respectively [26].

In this simulation, Smagorinsky [27] and one-equation models [28] are used as SGS. Magnussen and Hjertager presented the EDM combustion model in 1976, with the idea proposed by Spalding [19]. In this combustion model, the fuel consumption rate is calculated by Eq. (5):

$$\overline{\dot{\omega}''_F}=\bar{\rho}\frac{\min(\tilde{Y}_F,\tilde{Y}_{O_2}/s)}{\tau_{mix}}. \tag{5}$$

In Eq. (5), $\tilde{Y}_F,\tilde{Y}_{O_2}$, are the mass fractions of the oxidizing and the fuel, respectively, and s is the air-to-fuel stoichiometric mass ratio. τ_{mix} is the time scale of mixing which is obtained by Eq. (6):

$$\tau_{mix} = \min\left(\underbrace{\frac{k_{SGS}}{C_{EDM}\varepsilon_{SGS}}}_{\tau_{turb}}, \underbrace{\frac{\Delta^2}{C_{diff}\alpha}}_{\tau_{lam}}\right),$$

$$C_{EDM} = 4, \qquad C_{diff} = 4. \tag{6}$$

In Eq. (6), k_{SGS}, ε_{SGS} are mean turbulent kinetic energy and turbulent dissipation rate which are calculated from the SGS parameter. α is thermal diffusivity and Δ is the filter width in the LES method. The infinite fast chemistry model is based on the assumption that the reactions occur very quickly; in other words, the reaction takes place by the mixing of fuel and oxidizing. This means that the time scale of chemical reactions is much faster than the time scale of diffusion and flow transfer. In this case, the fuel reaction rate, which appears in the form of the fuel mass transport source term, can be modeled with Eq. (7):

$$\overline{\dot{\omega}''_F} = \bar{\rho}\frac{\min(\tilde{Y}_F, \tilde{Y}_O/s)}{C_c\Delta t}. \tag{7}$$

In Eq. (7), C_c, and Δt are the time step and constant coefficient of this model, respectively. In this simulation, for all examined states, the assumption of the irreversible single-step reaction is used.

Radiation heat transfer is modeled using the Discrete Ordinate Method (DOM). The interaction between the radiation and the SGS is ignored. In most studies of fire modeling, it is noted that for the radiation model, it is better to use S4 (8×3 space angles) and to use the upwind method to discretize the radiation equation [29].

2.1. Numerical method

For this simulation, the fireFoam solver of OpenFOAM (which is a free, open-source Computational Fluid Dynamic (CFD) software developed primarily by OpenCFD Ltd in 2004) has been used. FireFOAM is a C^{++}, object-oriented LES code based on OpenFOAM, which was developed by Factory Mutual (FM) Global. This solver uses the finite volume method [30], and the PIMPLE algorithm is used for taking into account the coupling of velocity and pressure [31]. Also, Rhie-Chow interpolation is used to avoid odd-even decoupling, and the pressure equation is solved by a linear generalized Geometric-Algebraic Multi-Grid (GAMG) solver.

The maximum local courant number is considered as 0.6, in which the time step is about 0.0005 seconds, in this case for 2000000 mesh. The second-order approximation is used for all convective terms in the equations of momentum, sub-grid turbulence kinetic energy, and energy equation. For the temporal term in all equations, the first order Eulerian method is chosen. The first order derivative of the radiation intensity in different directions is discretized by first-order upwind approximation.

Table 1. Different case used in the simulation.

Cases	SGS model	Combustion model
S-E*	Smagorinsky SGS	EDM
S-I	Smagorinsky SGS	Infinite fast chemistry
O-E	One-equation SGS	EDM
O-I	One-equation SGS	Infinite fast chemistry

* This state is considered as a reference case.

Two combustion models of EDM and infinite fast chemistry with two SGS models of Smagorinsky and one-equation are evaluated, in order to investigate the effect of the combustion model, as well as the compatibility of the combustion model with the SGS model, according to Table 1.

A computer system with a shared memory system and a 16 Intel-Core i5-2400 with frequencies of 3.1 GHz, which have four real kernel cores, and 4 GB of temporary memory is used. This machine could perform parallel processing with the MPI library of OpenFOAM code. In most computations, 12 cores are used for each study, at the same time. As an estimate, the computational time for the mentioned models is approximately 168 hours for 3 million grids for the modeling of pool fire behavior in 35 seconds (to achieve quasi-steady state) by 12 cores. Table 2 shows the computational cost of the implemented simulation for different grids (1000000, 2000000, and 3000000 grids).

2.2. Description of the experiment

The modeling is based on the test done by Tieszen et al. [32] for a methane pool fire with an inlet diameter of one meter. In [32] instantaneous velocity was measured by the PIV method on the central fire plane, and the turbulence parameters were reported. Vertical velocity was reported instantly for a point at 0.505 m above the fuel inlet. Finally, the average velocity and turbulence parameters in the central plate were presented. The accuracies of $\overline{u'^2}$, $\overline{v'^2}$ and $\overline{u'v'}$values are about ± 35%.

As indicated in Figure 1, a computational domain of $3 \times 3 \times 7$ m^3 was considered to simulate this test of a one-meter pool fire. The fuel is supplied from a circular inlet of one meter in diameter with $\dot{m}_{fuel} = 0.066$ kgm^{-2}s^{-1}. The boundary condition of temperature, velocity and species is Dirichlet for the fuel input area.

$$V_{inlet} = 0.117 \text{ m/s},$$

$$T_{inlet} = 274 \text{ K},$$

$$Y_{CH_4,inlet} = 1. \tag{8}$$

Bottom walls near the fuel inlet are considered as under a no-slip condition ($V_{wall} = 0.0$ m/s) and the boundary

Table 2. The computational cost for different grids (simulation time in these cases is 35 s).

Computational property/mesh size	1000000 grids	2000000 grids	3000000 grids
Number of cores	4	8	12
System's temporary memory (RAM)	3.6 GB	3.6 GB	3.6 GB
Processing power (CPU)	3.1 GHz	3.1 GHz	3.1 GHz
Computational time	95 h	160 h	168 h

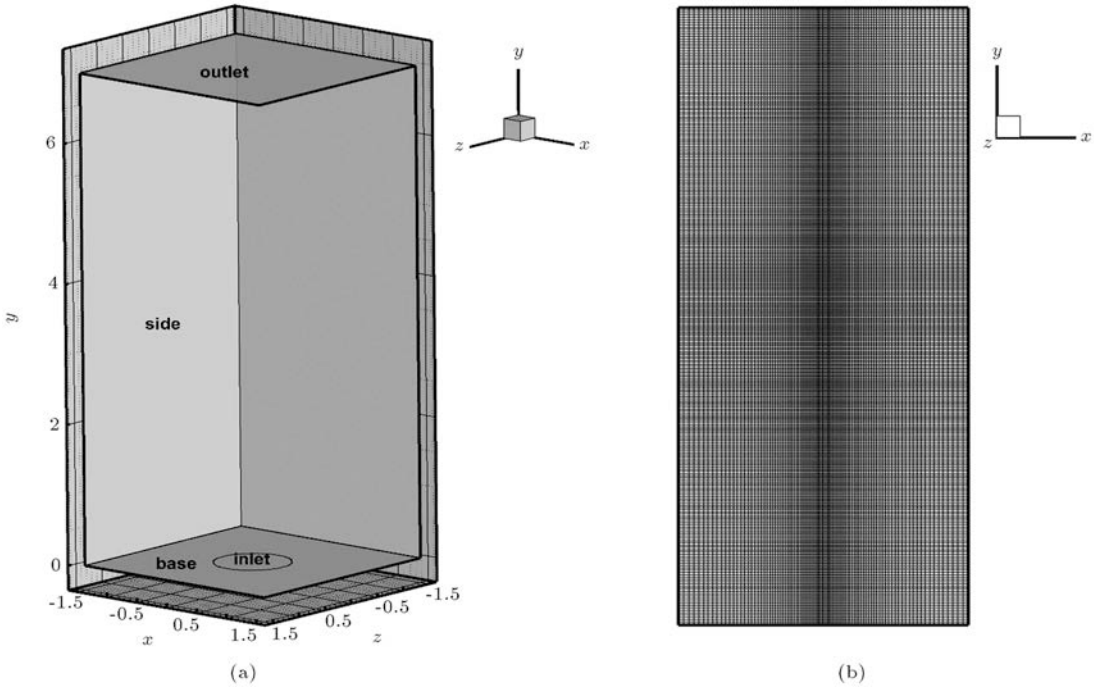

Figure 1. Computational domain of one-meter pool fire simulation: (a) General geometry dimensions and (b) a view of the mesh.

condition for temperature is adiabatic ($\partial T/\partial n = 0$). The outside pressure is 81 kPa and zero gradient ($\partial P/\partial n = 0$) at the base wall and fuel inlet. The temperature, velocity, pressure and species for initial value are considered as:

$$V_{initial} = 0 \text{ m/s},$$

$$T_{initial} = 278 \text{ K},$$

$$P_{initial} = 81 \text{ kPa},$$

$$Y_{\text{species, initial}} = Y_{air} \rightarrow Y_{O2} = 0.23,$$

$$Y_{N2} = 0.77, \qquad Y_{\text{other}} = 0. \tag{9}$$

The results should be averaged to compare with experimental data. Experimental results have been averaged over 11 cycles (equivalent to about 6 seconds). In this numerical study, the average period is about 20 seconds after the quasi-steady state behavior of the fire.

The proper length scale for fire plume and buoyancy flow is defined by Eq. (10):

$$L^{base} = \left(\frac{\dot{Q}_{comb}}{\rho_\infty T_\infty C_p \sqrt{g}}\right)^{0.4}. \tag{10}$$

This length scale is an estimate of the effective area around the pool fire which is affected by the combustion. This parameter is used as an estimate of the required computing grid. In general, large-scale values are properly resolved when at least ten computational grids are considered for this length scale [19]. In this modeling, the length scale is about 1.3 m, which is calculated from Eq. (8).

The flame Plume Resolution Index (PRI) is defined for achieving the required computational grid in a parametric fire model. According to this parameter, one can refer to the grid used in LES fire modeling. This parameter is defined as Eq. (11):

$$PRI = \frac{L^{base}}{\Delta x}. \tag{11}$$

In Eq. (11), Δx is the size of the computational grid.

For general modeling of the fire flow, it is usually recommended that the PRI value be between 5 and 15 [33]. However, for a detailed study of the oscillatory behavior, the PRI value should be greater than 40 [19]. In the present study, the PRI value is almost 55, so it presents the modeling details with high precision.

3. Results and discussions

3.1. Grid sensitivity

One of the concerns raised in the use of the LES method is the number of the required computational grid. In the previous section, a brief account of the computational grid number was stated. In this section, to investigate the effect of the computational grid on fire simulation results, the results of vertical velocity and vertical velocity fluctuation are evaluated.

In Figure 2(a) and (b), the results of the mean vertical velocity and mean squared of vertical velocity fluctuation are compared for three grid types of 1000000, 2000000, and 3000000 (each of the three grid types has the required PRI) in $y = 0.4$ m on the central plane ($z = 0$).

According to Figure 2, the results of the 2000000 and 3000000 grids are similar (the difference is less than 5%). To compare the results of various models of combustion and turbulence SGS, the 3000000 grid is selected. The results of this mesh in the simulation are investigated.

The PRI index is one of the fire-specific indexes. The other general index for verifying the computational grid is the LES_{IQ}. This index expresses the ratio of the amount of modeled turbulence kinetic energy to the total turbulence kinetic energy of the flow. Pope [34] proposed that in the simulation of the LES method, at least 80% of the turbulent kinetic energy must be solved directly. LES_{IQ} is defined as Eq. (12):

$$LES_{IQ} = \frac{k_{Resolved}}{\underbrace{k_{Resolved} + k_{SGS}}_{k_{total}}} \tag{12}$$

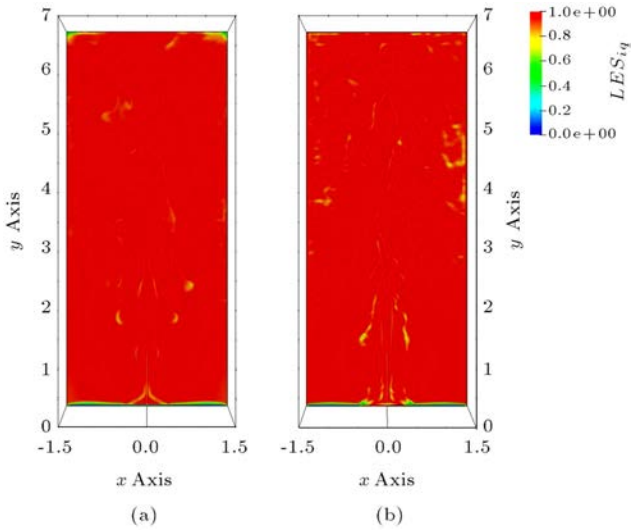

Figure 3. LES_{IQ} at the $z = 0$ for (a) O-E and (b) O-I.

In Eq. (12), $k_{Resolved}$ is the amount of turbulence kinetic energy which is directly modeled by the LES method and k_{SGS} is the kinetic energy of the SGS. In Figure 2(c), the results of LES_{IQ} are compared for three grid numbers of 1000000, 2000000, and 3000000 (which represent grids sizes 0.05, 0.032, and 0.025 m, respectively) in the $y = 0.4$ m on the central plane ($z = 0$). As can be seen, the results of a grid number of 1000000 starts at about 0.75 and approaches close to 0.97, but the results of the LES_{IQ} of the other two grids in almost the entire x-axis are greater than 0.9, which indicates the optimal accuracy of these grids. In Figure 3, LES_{IQ} is plotted at the $z = 0$ for the two cases O-E and O-I, the mesh number of which is 3000000. As observed, the index value of LES_{IQ} is higher than 80% in most points, illustrating the quality of the mesh required for this case.

3.2. Puffing phenomena

One of the most important phenomena that occur in the fire is called the puff phenomenon [35,36]. In fact, this phenomenon describes the appearance of vortices

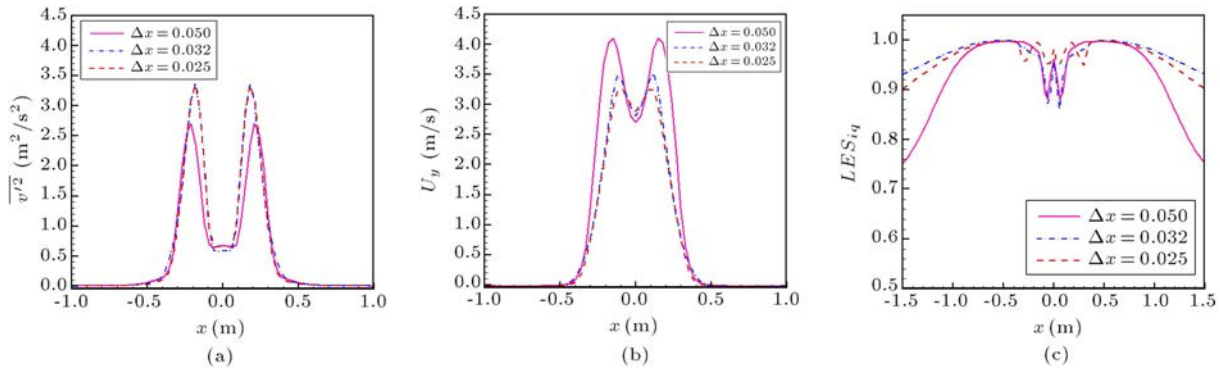

Figure 2. Results of mesh study: (a) Mean of vertical velocity, (b) mean squared of vertical velocity fluctuation, and (c) LES_{IQ}.

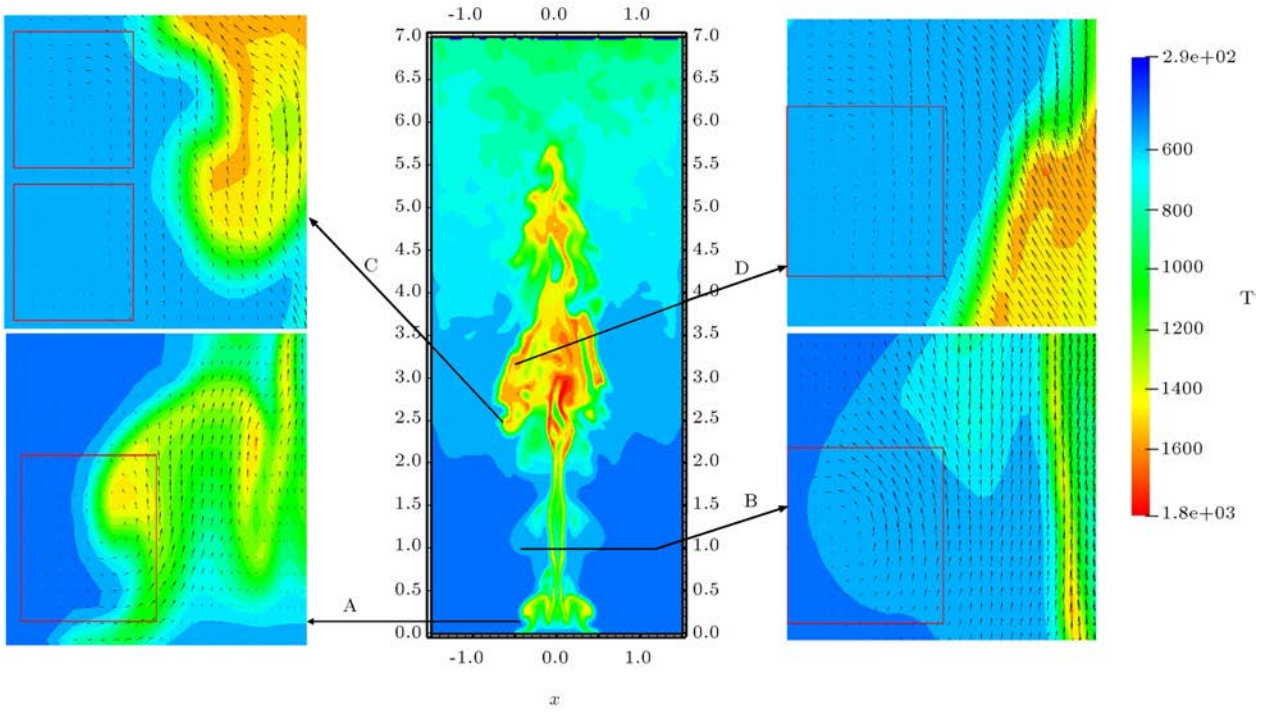

Figure 4. Cycle of formation and dissipation of Puffing vortex.

on the flame surface [37,38]. Due to the difference in density of the horizontal direction of the flame range, and on the other hand, the pressure difference, which is created in the vertical direction due to gravity, the baroclinic and gravity produce the Puffing vortex. This process can be seen in Figure 4. So, the small vortices are formed at the lower surface of the flame with the formation of flames.

These vortices move up the flame and grow on their path until they reach the upper surface of the flame then separate from the flame and dissipate.

This phenomenon causes oscillating behavior and instability at the flame surface. Moreover, it gradually creates a fluctuation in velocity, temperature, and turbulence parameter. In Figure 4, by using the temperature contour, as well as the velocity vector, the cycle of formation and dissipation of the puffing vortex (after reaching the quasi-steady state) is depicted. As shown in this figure (part A), a small vortex was initially created near the inlet due to the difference in flow density in the horizontal direction and the pressure difference in the vertical direction [39].

By decreasing the density of the mixture relative to the environment, the buoyancy force is activated which is corresponding to the difference of the density of the mixture and the surrounding environment. Thus, the hot gases generated by the combustion move upward due to buoyancy forces and get bigger along their path (part B). Vortices while moving upward, merge (part C) and form a larger vortex (part D). So, the combustion gradually disappears, the energy that has been transferred to the vortices is dissipated, and gradually vortices disappear (the end of the fire).

3.3. Puffing frequency

In the modeling of pool fire with the LES method, the results are changed periodically, because of the puffing phenomenon. The experimental results [32] reported the instantaneous velocity variation at the height of 0.505 m from the fuel inlet in the central line ($x = z = 0$). The experimental puffing frequency is about 1.65 Hz, at this point.

The dominant frequencies of the oscillating flow are extracted with Fast Fourier Transform (FFT) analyses to evaluate the puffing frequency. Figure 5 shows the frequency analysis of vertical velocity data using different methods (for the point at the height of 0.505 m). According to the figure, the dominant frequency, representing the puffing frequency, is given in Table 3.

The infinite fast chemistry combustion model has

Table 3. Puffing Frequency of different cases.

Frequency	Experimental [32]	O-I	O-E	S-I	S-E
Puffing frequency (Hz)	1.65	1.93	1.83	1.90	1.86
Error	–	17%	11%	15%	13%

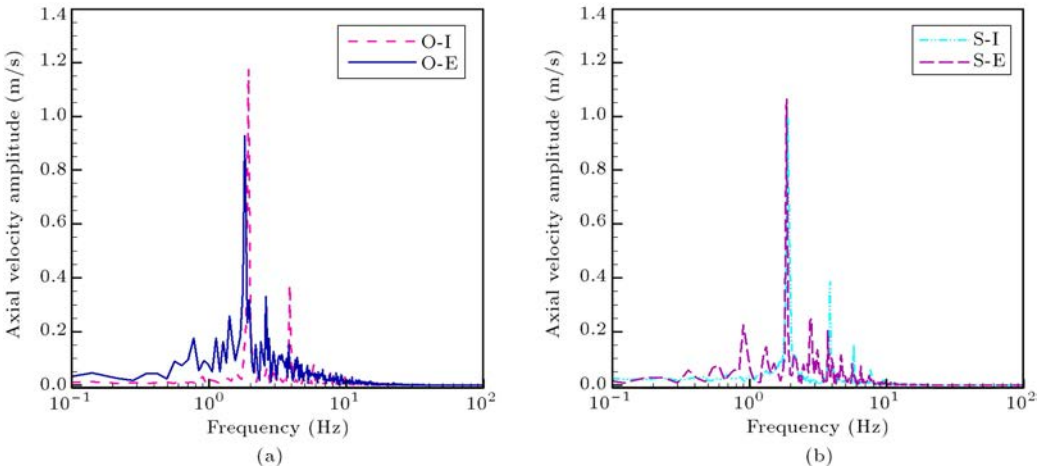

Figure 5. Frequency analysis of vertical velocity data at 0.505 m height of the center line ($x = z = 0$): (a) One-equation Sub-Grid Scale (SGS) and (b) Smagorinsky SGS.

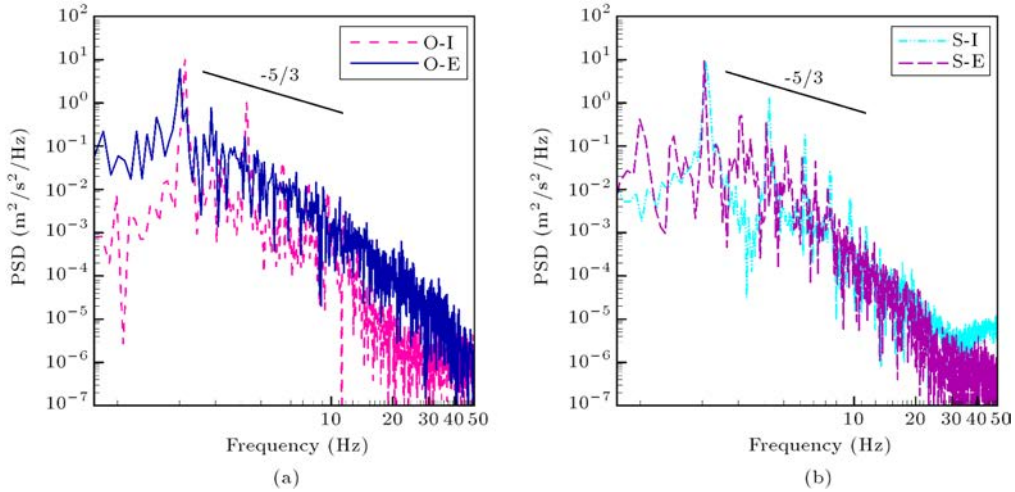

Figure 6. Power Spectral Density (PSD) frequency analysis of vertical velocity data at 0.505 m height of center line ($x = z = 0$): (a) One-equation SGS and (b) Smagorinsky Sub-Grid Scale (SGS).

a lower accuracy in Smagorinsky and one-equation SGS for the prediction of puffing frequency. In contrast, the EDM combustion model has given puffing frequency more precisely. When the EDM combustion model is used with a one-equation SGS, the puffing frequency has 11% relative error from experimental results, although the accuracy of this combustion model is lower in the case of using the Smagorinsky SGS.

In general, numerical models report higher frequencies than experimental results. Because these combustion models are based on fast kinetics and predict the amount of heat release more than reality, by releasing too much energy, the gas velocity increases, and the puffing vortex moves up faster. So, the value of the puffing frequency increases accordingly.

The LES model is based on the assumption that the large vortices are solved directly and the effects of small vortices are modeled with SGS models [40]. The energy of large scale vortices gradually transfers into smaller vortices, until they eventually turn into vortices known as Kolmogorov and, then, dissipate their energy. This vortex energy transformation from large scale vortices to those of Kolmogorov is called energy cascade.

Figure 6 shows the results of the energy spectrum versus frequency at the point at a 0.505 m height of the center line ($x = z = 0$). As shown in Figure 6, the magnitude of the Power Spectral Density (PSD) increases at frequencies in which the velocity amplitude increases in the FFT graph (Figure 5). Then, the PSD value reaches its maximum value at the puffing frequency. Therefore, the values of PSD and velocity amplitude are maximum at the puffing frequency.

Taylor-scale vortices are in the area where energy is transmitted from large vortices to small-scale vortices [41]. Within this area, the energy spectrum has a power functional of $-5/3$ of the wave number that is proportional to the inverse of the vortex length or the

Table 4. The position of the four points on the central line ($x = z = 0$) in the y direction to compute the Power Spectral Density (PSD).

	A	B	C	D
Point position	$x = z = 0$, $y = 0.2$ m	$x = z = 0$, $y = 1.5$ m	$x = z = 0$, $y = 3.0$ m	$x = z = 0$, $y = 6.0$ m

frequency. In Figure 6, the $-5/3$ slope is shown; as can be seen, the slopes of the PSD lines in two combustion models are almost close to the $-5/3$ slope, although somewhere the slope is more than $-5/3$.

For a better evaluation of energy cascade in pool fire, four points with positions along the center line of the domain are selected. In Table 4, the positions of these four points of reference, case (O_E) on the central line ($x = z = 0$) perpendicular to the fuel bed, are given. The arrangement of these points is such that it covers the formation of the puffing vortices until their dissipation, and in fact, these four points are key points in the puffing formation cycle. Point A is in the vicinity of the fuel bed, where the puffing vortex is formatted. The difference of density in the horizontal direction and the pressure difference in the vertical direction is the most important factor in the formation of the puffing vortex. At this point (point A), the puffing vortex has a small size, and it moves upward (due to the buoyancy force) and gradually becomes larger by receiving combustion energy (point B). When the puffing vortex reaches the midpoint of the flame (point C), there are several vortices that have formed near the fuel bed and moved upwards. Therefore, these vortices merge together and form a larger vortex.

In Figure 7, the frequency analyses of these four points are shown. According to Figure 7(a), the dominant frequency of point A (f_A) is the frequency of vortex that forms near the fuel bed. Then, the vortex goes up to reach point B, while its frequency does not change in this path (i.e., $f_B = f_A$). However, according to Figure 7(c), the amount of kinetic energy associated with this frequency increases, due to the energy received from the combustion process. As seen in Figure 7(b), by reaching point C, two dominant vortices with f_{C1} and f_{C2} frequencies are merged. So, only a vortex with a dominant frequency of f_D can be observed at point D.

According to Figure 7(c), from points A to C, the level of energy received has increased. From point C to point D, the amount of intake energy decreases. At the height between points C and D, the amount of energy released by combustion reduces and, also, the vortices begin to dissipate. In Figure 4, this behavior can also be observed schematically.

3.4. Comparison of the turbulence field

One of the issues in the investigation of the turbulence field using the LES modeling is the calculation of parameters such as fluctuation velocity, mean squared of velocity fluctuation, and turbulence kinetic energy. The main problem in computing these parameters is that in the LES modeling the filtered parameters are calculated and these parameters differ from instantaneous parameters such as instantaneous velocity, which results from the SGS.

In [32], the mean square curve of the horizontal and vertical velocity fluctuations and turbulence kinetic energy on the middle plate ($z = 0$), was reported for a one-meter pool fire. According to Eqs. (13) and (14), the relation between two turbulence kinetic energies, one of which is calculated from an instantaneous velocity, and the other using the LES method, is given. In the LES method, k_{SGS} is calculated using the assumption of the local equilibrium between production and energy dissipation in the SGS. The total turbulence kinetic energy is calculated according to Eq. (14):

$$k_{resolved} = \frac{1}{2}\overline{(\tilde{u}_i - \bar{u}_i)^2}, \tag{13}$$

$$k_{total} = k_{resolved} + k_{SGS}. \tag{14}$$

For calculation of $k_{resolved}$ in Eq. (13), $(\tilde{u}_i - \bar{u}_i)$ is used to determine velocity fluctuations, then the square of velocity fluctuation values are averaged around 20 seconds. To calculate the sub-grid velocity fluctuations in Eq. (15), isotropic sub-grid velocity fluctuation is assumed. An estimated value of sub-grid velocity fluctuations is obtained according to Eq. (16):

$$\overline{u'^2_i} = \overline{(u_i - \bar{u}_i)^2} = \overline{((\tilde{u}_i - \bar{u}_i) + (u_{SGS})_i)^2}$$
$$= \overline{(\tilde{u}_i - \bar{u}_i)^2} + \overline{(u_{SGS})_i^2}, \tag{15}$$

$$(u_{SGS})_1 = (u_{SGS})_2 = (u_{SGS})_3$$
$$= \sqrt{\left(\frac{2}{3}k_{SGS}\right)} \rightarrow \overline{u'^2_i} = \overline{(\tilde{u}_i - \bar{u}_i)^2} + \overline{\left(\frac{2}{3}k_{SGS}\right)}. \tag{16}$$

In Figure 8, the mean square values of the horizontal, vertical fluctuation velocity and turbulence kinetic energy are given at two heights of 0.4 and 0.8 m (in $z = 0$ plane). For investigating the effect of sub-grid velocity fluctuations on the results, the mean square of the fluctuations velocity and turbulence kinetic energy are compared in two modes with and without the effect of the sub-grid velocity fluctuations.

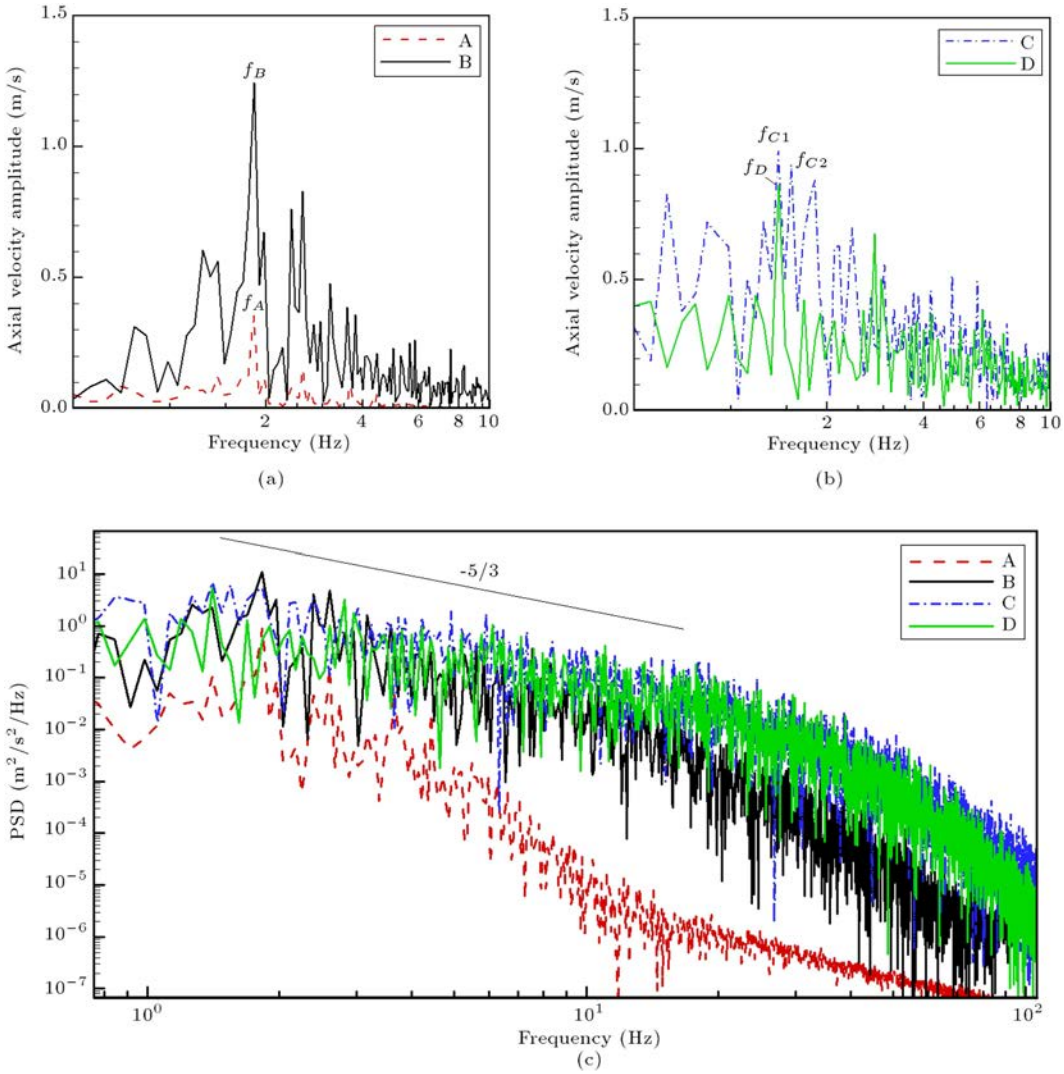

Figure 7. Frequency analysis of vertical velocity data in (a) points A and B, (b) points C and D, and (c) Power Spectral Density (PSD) results at points A, B, C and D.

As can be seen in Figure 8, the value of the sub-grid velocity fluctuations is relatively small with respect to the velocity fluctuation. Hence, the mean squared of vertical velocity fluctuation and turbulence kinetic energy is the same in the two cases and at two heights of 0.4 and 0.8 m, which means that the sub-grids velocity fluctuations do not have much effect on these parameters. However, the sub-grid velocity fluctuation affects the mean squared of the horizontal velocity fluctuations (although it has a small effect). The reason is that the mean square fluctuation of the horizontal velocity is smaller than the mean square of the vertical velocity fluctuation, and therefore, even the small amount of sub-grid velocity fluctuation can affect it.

3.5. Comparison of mean squared fluctuation of velocity

In Figure 9, the results of the comparison of the mean square fluctuation of horizontal velocity in two sections $Y = 0.4$ and 0.8 m ($Z = 0$ plane) are presented. According to the experimental results, the mean square fluctuation of horizontal velocity at two tails of the curve approach to zero, due to the fact that the flow is laminar. But as one reaches close to the center ($X = 0$), the mean square fluctuation of horizontal velocity approaches its maximum value and again decreases at the center. It is due to the reduction of the horizontal velocity. In different examined cases, this process is observed in simulation, but the results of all these models are less than the experimental results. Among these four cases, at the height of 0.4, the case using an infinite fast chemistry combustion model is closer to the experimental values. But at the height of 0.8, the case that uses the EDM combustion model is closer to the experimental values. Among the cases that use the EDM combustion model, the O-E case has higher accuracy.

In Figure 10, the comparison of the mean square

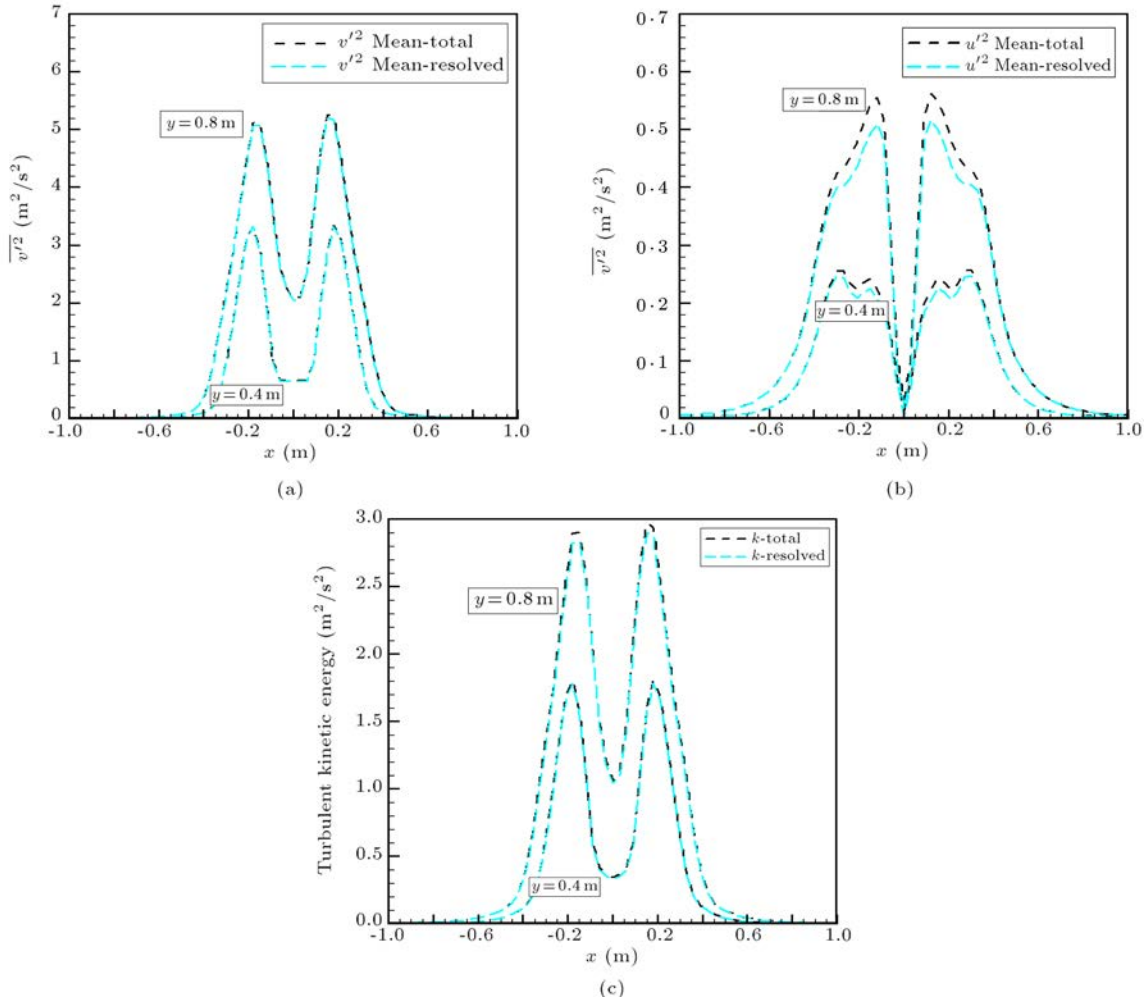

Figure 8. Comparison of (a) $\overline{v'^2}$, (b) $\overline{u'^2}$, and (c) turbulence kinetic energy with and without sub-grids velocity fluctuations effect.

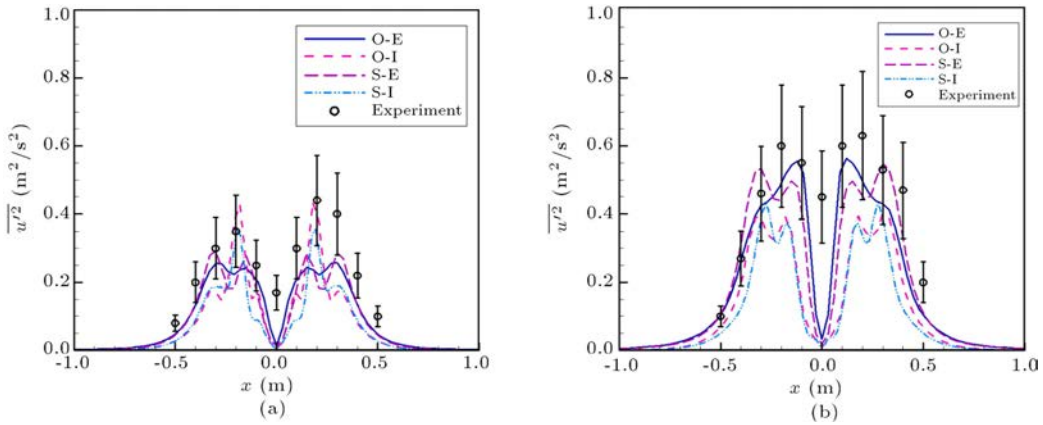

Figure 9. Comparison of the mean square fluctuations of horizontal velocity results at the height of (a) 0.4 m and (b) 0.8 m.

fluctuation of vertical velocity in two sections $y = 0.4$ and 0.8 m ($z = 0$ plane) are presented. The mean square fluctuation of vertical velocity results, such as the mean square fluctuation of horizontal velocity, at two tails of the curve, is close to zero. But, as the center ($x = 0$) is approached, it first increases, then decreases until it reaches its minimum in the center. Different cases (O_E, O_I, S_E, S_I) exhibit this trend, but the results of all these cases are greater than experimental results. Among these four cases, the models that use

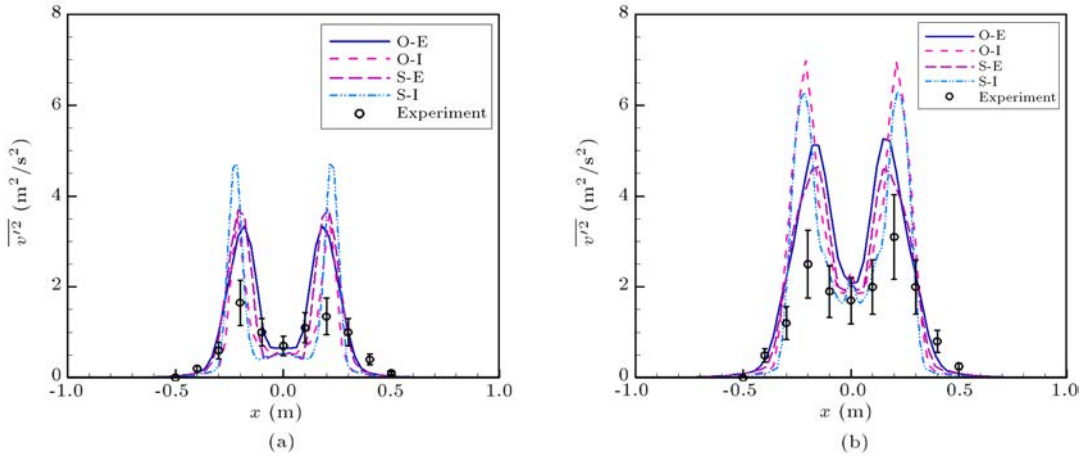

Figure 10. Comparison of the mean squared of vertical velocity fluctuation at the height of (a) 0.4 m and (b) 0.8 m.

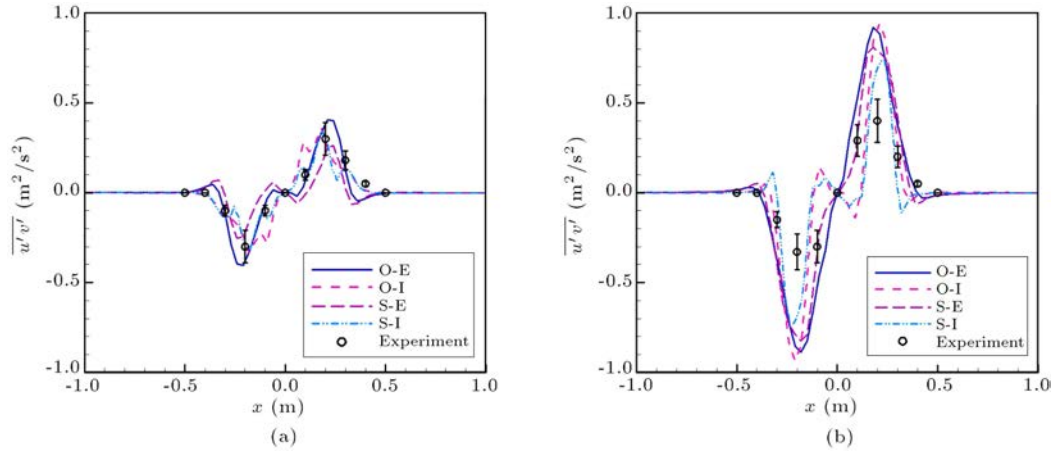

Figure 11. Comparison of $\overline{u'v'}$ at height of (a) 0.4 m and (b) 0.8 m.

the infinite fast chemistry combustion model, predict results which are greater than experimental results, but the results predicted by the EDM combustion model are closer to experimental values.

In Figure 11, $\overline{u'v'}$ were compared at two heights of $y = 0.4$ and 0.8 m (in $z = 0$ plane). $\overline{u'v'}$ exhibit a different behavior of the mean square of the vertical and horizontal fluctuation velocities, i.e. $u'v'$ is positive in one direction, in which both of u', v' are marked and $\overline{u'v'}$ is negative in the other direction where they are not marked. But $u'v'$ at two tails of the curve is close to zero due to the laminar flow. As the center ($x = 0$) is approached, $\overline{u'v'}$ first increases then decrease to zero at the center. Different models follow this trend, but the results of all these models are greater than predicted by the experimental results. Among these four cases, models that use an infinite fast chemistry combustion model have more over-prediction.

In general, flow is expected to be laminar in a region far from fire flames, and therefore, the velocity fluctuations are minimal. By approaching the region of flames, the areas of turbulence and the fluctuations appear. When one gets closer to the center of the flame, the amount of turbulence energy decreases.

In summation, it can be seen that in predicting the values of turbulence parameters, the infinite fast chemistry model has an over-prediction of the turbulence parameters. The turbulence SGS models do not have much effect on the results. However, the one-equation SGS has more accurate results. In fact, the effect of the combustion model is more dominant than the turbulence SGS models. Further, the other point is that nearly all models correctly predict the locations of the maxima or minima of the mean squared fluctuations velocity, but the results have been modeled by differences. The other point is that the farther from the fuel bed (at heights of 0.4 and 0.8), the amount of fluctuations increases, due to combustion intensification.

3.6. Comparison of turbulence kinetic energy results

In Figure 12, the results of the mean turbulence kinetic energy at two heights of $y = 0.4$ and 0.8 m (in

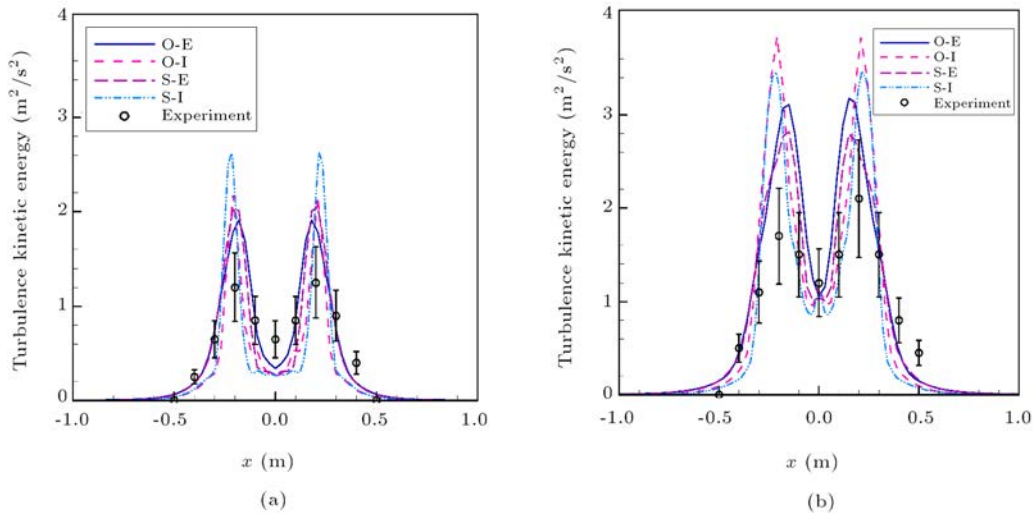

Figure 12. Comparison of the mean turbulence kinetic energy at the height of (a) 0.4 m and (b) 0.8 m.

$z = 0$ planes) are presented for different cases. In the experimental results [32], the mean turbulence kinetic energy was calculated with the assumption that $\overline{w'^2} = \overline{v'^2}$. Although in numerical calculations it is possible to calculate the direct mean turbulence kinetic energy, as an experimental result, the assumption $\overline{w'^2} = \overline{v'^2}$ was used in this simulation.

Due to the dominance of the perturbation in this direction, the mean turbulence kinetic energy follows the mean square of the vertical velocity fluctuation. The trend of variation in the mean turbulence kinetic energy at two tails of the curve goes to zero, due to the laminar flow. As the center ($x = 0$) is approached, mean turbulence kinetic energy first increases, then decreases in the center due to the reduction of combustion energy. According to Figure 12, different models follow this trend, but the results of all these models are greater than the experimental results. Among these four cases, those using the infinite fast chemistry combustion model are farther from experimental results than the others. But, the results predicted by the EDM combustion model are closer to experimental values.

Prediction of the numerical method results depends on the nature of the two combustion models. The infinite fast chemistry combustion model undertakes modeling with the assumption that combustion is implemented completely, as soon as the fuel and oxidizer are encountered. Then, reaction accrues according to the irreversible stoichiometry reaction. In this model, combustion predictions become further than the actual values. Therefore, the released energy increases and as a result, the turbulence becomes more apparent. However, the EDM combustion model accounts the characteristic time of the fuel and oxidizer mixing in the process of combustion, to improve the combustion results.

3.7. Influence of combustion model constant

Considering the results of the two combustion models and turbulence SGS in the previous sections, the EDM combustion model has much better results than the infinite fast chemistry combustion model. Therefore, in this section, by examining the coefficients of the EDM combustion model, the effect of these coefficients on the accuracy of the results has been examined. In general, two combustion models used estimate the fuel consumption to be high, and the coefficients need to be corrected for use in the pool fire. One of the methods that can be used to correct the combustion model is the correction of the coefficients according to the flow regime. In [23], by examining a small-scale methanol pool fire, the optimal EDM model constant is proposed to be one in a small-scale pool fire.

As indicated in Eq. (6), the default value of this coefficient is 4. As seen in the results of the previous section, the values of the turbulence parameter are somewhat higher than the experimental results, due to excessive combustion prediction. Therefore, in order to reduce the number of combustion parameters, the EDM combustion model must be reduced to decrease the combustion rate of the fuel; so one can reduce the amount of released energy and consequently, the turbulence parameters. In this modeling, by evaluating three coefficients 1, 2 and 4, the coefficient influence on the EDM combustion model is presented in the modeling of the turbulence parameters in a large scale pool fire of methane.

In Figures 13 and 14, the effect of the coefficients of the EDM combustion model on two cases, O_E and S_E, are investigated by changing the coefficients between 1–4. According to Figures 13 and 14, the change in coefficients does not have much effect on the mean square of horizontal velocity fluctuations. In fact, the EDM model is not able to predict the exact

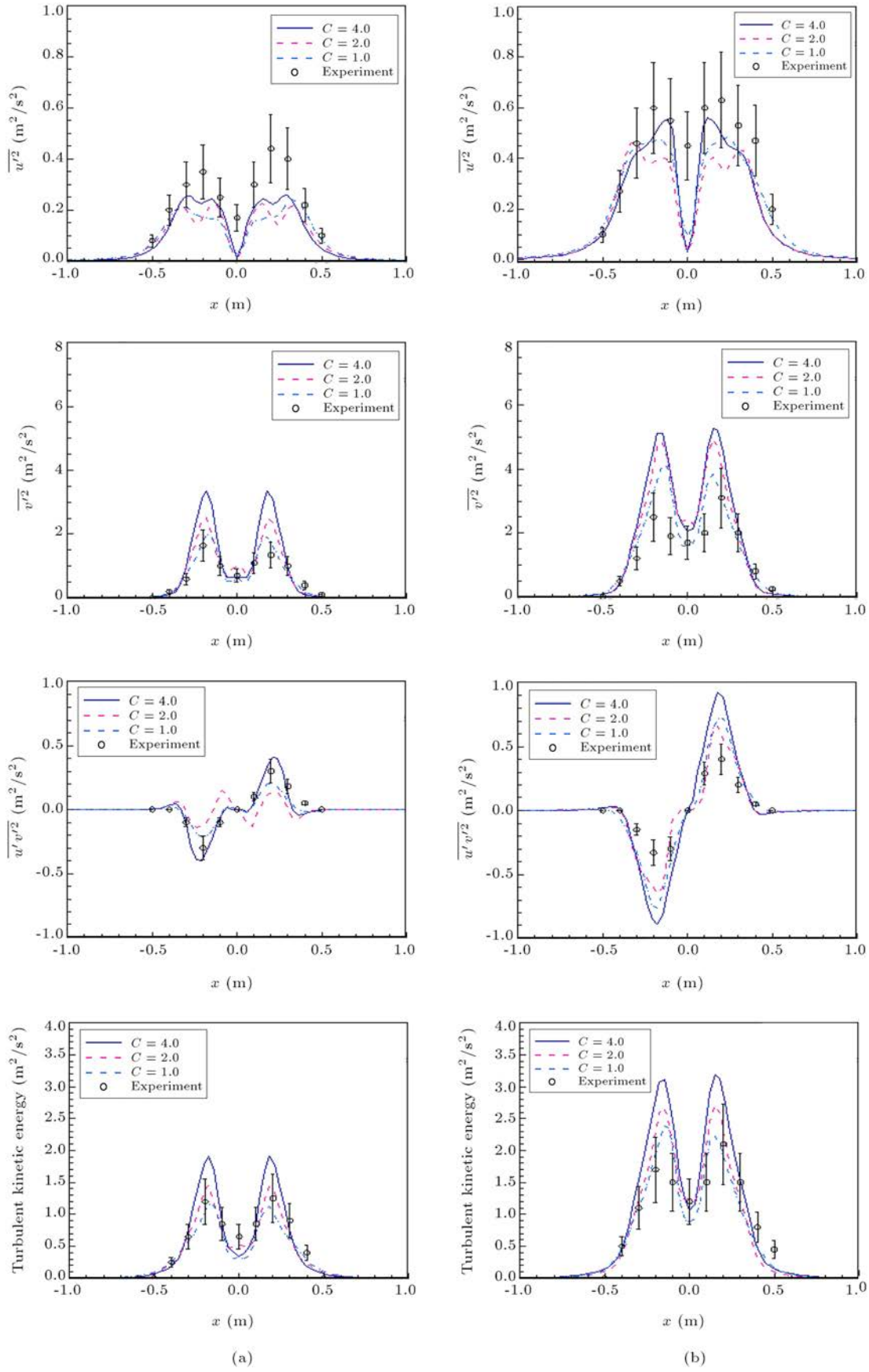

Figure 13. Comparison of different EDM_{constant} in case of O-E at the height of (a) $y = 0.4$ m and (b) $y = 0.8$ m.

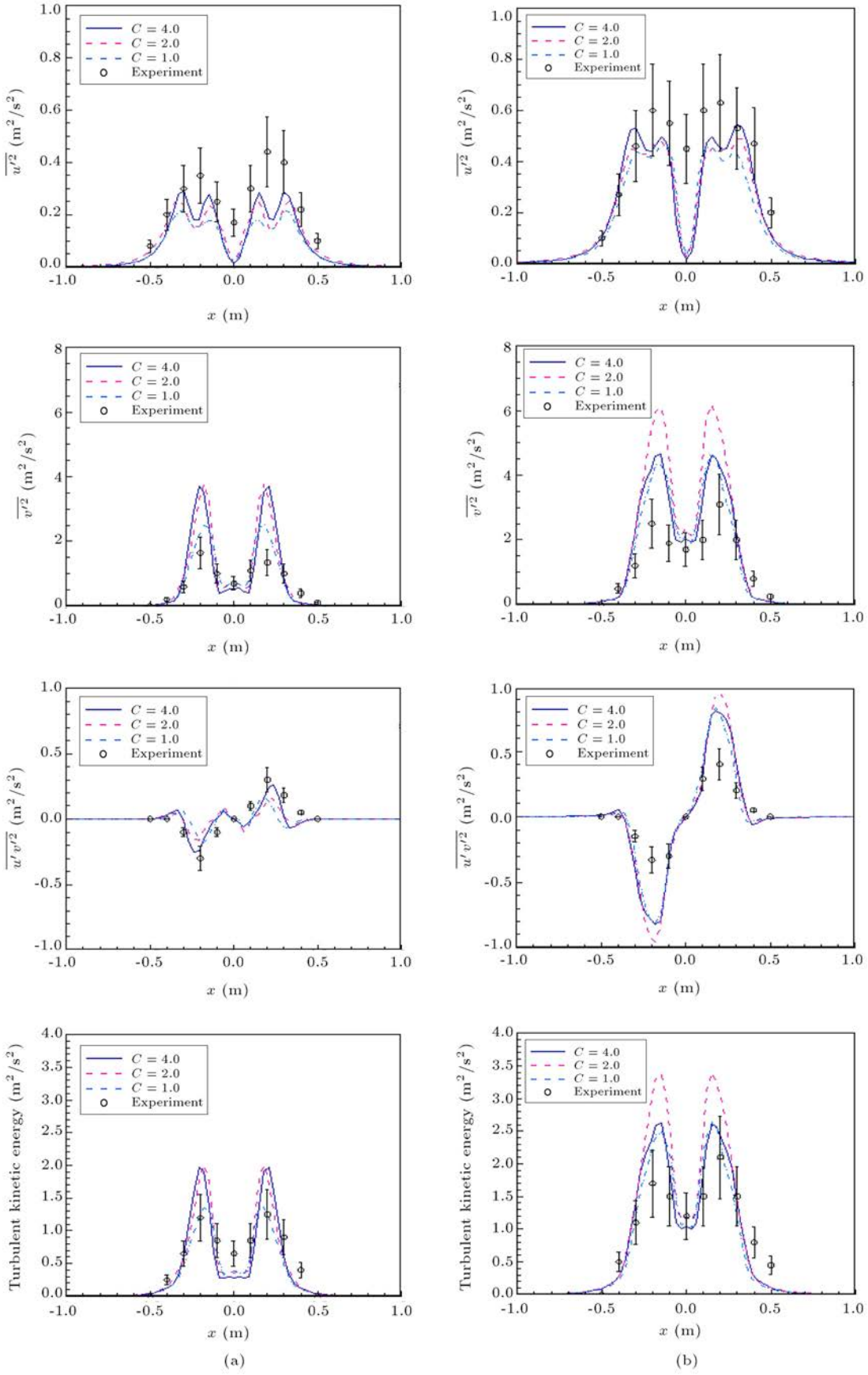

Figure 14. Comparison of different EDM_{constant} in case of S-E at the height of (a) $y = 0.4$ m and (b) $y = 0.8$ m.

mean square of the horizontal velocity fluctuation. If the coefficient one is used, the mean squared values of the vertical velocity, turbulence kinetic energy and $\overline{u'v'}$ are in an acceptable range with the experimental results. So in general, the coefficient 1 is the optimal EDM model constant.

A review of the results shows that although the coefficients of the combustion model reduced, the accuracy of the numerical results is closer to the experimental results; however, the use of other combustion models also can improve the numerical results. For example, the use of a Steady Laminar Flamelet Model (SLFM) or a Flamelet Generated Model (FGM) are two of these models [3].

4. Conclusion

The aim of this study is the investigation of the effects of infinite fast chemistry and Eddy Dissipation Model (EDM) combustion models on the accuracy of large pool fire numerical simulation. To investigate the compatibility of combustion models with the turbulence Sub-Grid Scale (SGS) models, two combustion models with two Smagorinsky and one equation SGS models were used. According to the results obtained in predicting the values of the turbulence parameter, the results of the infinite fast chemistry combustion model are greater than those of the EDM model. The turbulence SGS models do not have a significant effect on the results when used with two combustion models. In fact, the effect of the combustion model on the results is dominant. However, the results of a one-equation SGS model are more accurate than the Smagorinsky SGS model. The EDM combustion model has better compatibility with a one-equation SGS model. Further, nearly all models correctly predict the locations where the mean squared values of the velocity fluctuations are maximal or minimum. In general, the prediction of the results of the numerical turbulence parameters depends on the nature of the two models of combustion. The infinite fast chemistry combustion model undertakes modeling with the assumption that combustion is implemented completely, as soon as the fuel and oxidizer are encountered. In this model, combustion predictions become more than the actual values. Therefore, the released energy increases and as a result, the turbulence becomes more apparent. However, the EDM combustion model accounts for the characteristic time taken for the fuel and oxidizer mixing in the process of combustion, to improve the combustion results.

Nomenclature

c_p	Specific heat, J/kg. K
C_s	Smagorinsky constant
CFD	Computational Fluid Dynamic
D	Derivative
dt	Time step, s
g	Gravity, m/s^2
k	Turbulence kinetic energy, m^2/s^2
LES	Large Eddy Simulation
p	Pressure, kPa
Pr	Prandtl number
q_i	Diffusion/flux vector
S	Source term
S_{ij}	Rate of strain tensor, s^{-1}
SGS	Sub-Grid Scale
Sc	Schmidt numbers
T	Temperature, K
t	Time, s
u	Velocity, m/s
x	Coordinate, m
z	Mixture fraction

Greek symbol

Δ	Sub-grid length scale, m
δ_{ij}	Dirac delta function
μ	Molecular viscosity, kg/m.s
ν	Kinematic viscosity, m^2/s
ρ	Density, kg/m^3
τ_{ij}	Viscous stress tensor, kg/m.s
τ_{ui_T}	Turbulent diffusion/flux vector, kg/s^3
$\tau_{u_i u_j}$	Turbulent viscous stress tensor, kg/m.s
τ_{ui_φ}	Turbulent mass flux, kg/m^2.s
φ	Scalar quantity such as species
ω_T	Combustion heat release rate

Subscripts

i, j, k	Space index
Ref	Reference
t	Turbulence

Superscripts

$\sim$	Favre filtering
SGS	Sub-Grid Scale

References

1. Maragkos, G., Beji, T., and Merci, B. "Towards predictive simulations of gaseous pool fires", *Proceedings of the Combustion Institute*, **37**, pp. 3927–3934 (2019).
2. Ahmadi, O., Mortazavi, S.B., Pasdarshahri, H., and Mohabadi, H.A. "Consequence analysis of large-scale pool fire in oil storage terminal based on computational

fluid dynamic (CFD)", *Process Safety and Environmental Protection*, **123**, pp. 379–389 (2019).

3. Razeghi, S.M.J., Safarzadeh, M., and Pasdarshahri, H. "Comparison of combustion models based on fast chemistry assumption in large eddy simulation of pool fire", *Journal of the Brazilian Society of Mechanical Sciences and Engineering*, **42**, pp. 1–15 (2020).
4. Yuen, A., Yeoh, G., Timchenko, V., and Barber, T. "LES and multi-step chemical reaction in compartment fires", *Numerical Heat Transfer, Part A: Applications*, **68**, pp. 711–736 (2015).
5. Le, D.Q. "Numerical investigation of multi-compartment fire scenarios using Large Eeddy Simulation (LES)", Master's Thesis, University of Waterloo (2016).
6. Zou, G. and Chow, W. "Generation of an internal fire whirl in an open roof vertical shaft model with a single corner gap", *Journal of Fire Sciences*, **33**, pp. 183–201 (2015).
7. Chow, W. and Yin, R. "A new model on simulating smoke transport with computational fluid dynamics", *Building and Environment*, **39**, pp. 611–620 (2004).
8. Assad, M. "Improved fire modelling", PhD Theses, The University of Manchester (United Kingdom) (2014).
9. McGrattan, K., Rehm, R., and Baum, H. "Fire-driven flows in enclosures", *Journal of Computational Physics*, **110**, pp. 285–291 (1994).
10. Byström, A., Cheng, X., Wickström, U., and Veljkovic, M. "Measurement and calculation of adiabatic surface temperature in a full-scale compartment fire experiment", *Journal of Fire Sciences*, **31**, pp. 35–50 (2013).
11. Chiew, H.Z. "Fire dynamics simulation (FDS) study of fire in structures with curved geometry", PhD Theses, UTAR (2013).
12. Marchand, A., Verma, S., White, J., Marshall, A., Rogaume, T., Richard, F., Luche, J., and Trouvé, A. "Simulations of a turbulent line fire with a steady flamelet combustion model and non-gray gas radiation models", In *Journal of Physics: Conference Series*, p. 042009 (2018).
13. Chow, W., Dang, J., Gao, Y., and Chow, C. "Dependence of flame height of internal fire whirl in a vertical shaft on fuel burning rate in pool fire", *Applied Thermal Engineering*, **121**, pp. 712–720 (2017).
14. Xue, H., Ho, J., and Cheng, Y. "Comparison of different combustion models in enclosure fire simulation", *Fire Safety Journal*, **36**, pp. 37–54 (2001).
15. Huang, Y.-L., Shiu, H.-R., Chang, S.-H., Wu, W.-F., and Chen, S.-L. "Comparison of combustion models in cleanroom fire", *Journal of Mechanics*, **24**, pp. 267–275 (2008).
16. White, J., Vilfayeau, S., Marshall, A., Trouve, A., and McDermott, R.J. "Modeling flame extinction and reignition in large eddy simulations with fast chemistry", *Fire Safety Journal*, **90**, pp. 72–85 (2017).
17. Yeoh, G., Yuen, R., Chueng, S., and Kwok, W. "On modelling combustion, radiation and soot processes in compartment fires", *Building and Environment*, **38**, pp. 771–785 (2003).
18. Yang, D., Hu, L., Jiang, Y., Huo, R., Zhu, S., and Zhao, X. "Comparison of FDS predictions by different combustion models with measured data for enclosure fires", *Fire Safety Journal*, **45**, pp. 298–313 (2010).
19. Maragkos, G. and Merci, B. "Large Eddy simulations of CH4 fire plumes", *Flow, Turbulence and Combustion*, **99**, pp. 239–278 (2017).
20. Pasdarshahri, H., Heidarinejad, G., and Mazaheri, K. "Large eddy simulation on one-meter methane pool fire using one-equation sub-grid scale model", In *MCS*, pp. 11–15 (2012).
21. Yuen, A., Yeoh, G., Timchenko, V., Cheung, S., and Chen, T. "Study of three LES subgrid-scale turbulence models for predictions of heat and mass transfer in large-scale compartment fires", *Numerical Heat Transfer, Part A: Applications*, **69**, pp. 1223–1241 (2016).
22. Yuen, A.C., Yeoh, G.H., Timchenko, V., Cheung, S.C., Chan, Q.N., and Chen, T. "On the influences of key modelling constants of large eddy simulations for large-scale compartment fires predictions", *International Journal of Computational Fluid Dynamics*, **31**, pp. 324–337 (2017).
23. Maragkos, G., Beji, T., and Merci, B. "Advances in modelling in CFD simulations of turbulent gaseous pool fires", *Combustion and Flame*, **181**, pp. 22–38 (2017).
24. Echekki, T. and Mastorakos, E., *Turbulent Combustion Modeling: Advances, new Trends and Perspectives*, Springer Science & Business Media (2010).
25. Knio, O.M., Najm, H.N., and Wyckoff, P.S. "A semi-implicit numerical scheme for reacting flow: II. Stiff, operator-split formulation", *Journal of Computational Physics*, **154**, pp. 428–467 (1999).
26. Poinsot, T. and Veynante, D. "Theoretical and numerical combustion" RT Edwards, Inc. (2005).
27. Zhang, L., Deng, J., Sun, W., Ma, Z., Su, G., and Pan, L. "Performance analysis of natural convection in presence of internal heating, strong turbulence and phase change", *Applied Thermal Engineering*, **178**, p. 115602 (2020).
28. Moser, R.D., Haering, S.W., and Yalla, G.R. "Statistical properties of subgrid-scale turbulence models", *Annual Review of Fluid Mechanics*, **53**, pp. 255–286 (2020).
29. Da Costa, P.P.S. "Validation of a mathematical model for the simulation of loss of coolant accidents in nuclear power plants", Master Thesis, Department of Mechanical Engineering, Técnico Lisboa, Portugal (2016).
30. Singh, P.K. "Performance comparison of finite volume method and lattice Boltzmann method", Internship Report (2020).

31. Fancello, A.A., *Dynamic and Turbulent Premixed Combustion Using Flamelet-Generated Manifold in OpenFOAM*, BOXPress (2014).

32. Tieszen, S., O'hern, T., Schefer, R., Weckman, E., and Blanchat, T. "Experimental study of the flow field in and around a one meter diameter methane fire", *Combustion and Flame*, **129**, pp. 378–391 (2002).

33. Yeoh, G.H., Cheung, S.C.P., Tu, J.Y., and Barber, T.J. "Comparative large eddy simulation study of a large-scale buoyant fire", *Heat and Mass Transfer*, **47**(9), pp. 1197–1208 (2011).

34. Pope, S.B. "Ten questions concerning the large-eddy simulation of turbulent flows", *New Journal of Physics*, **6**, p. 35 (2004).

35. Jiang, X. and Luo, K. "Spatial direct numerical simulation of the large vortical structures in forced plumes", *Flow, Turbulence and Combustion*, **64**, pp. 43–69 (2000).

36. Jiang, X. and Luo, K. "Mixing and entrainment of transitional non-circular buoyant reactive plumes", *Flow, Turbulence and Combustion*, **67**, pp. 57–79 (2001).

37. Khrapunov, E. and Chumakov, Y. "Unsteady processes in a natural convective plume", In *Journal of Physics: Conference Series*, **1038**(1), p. 012132 (2018).

38. Maynard, T. and Princevac, M. "The application of a simple free convection model to the pool fire pulsation problem", *Combustion Science and Technology*, **184**, pp. 505–516 (2012).

39. De Ris, J.L. "Mechanism of buoyant turbulent diffusion flames", *Procedia Engineering*, **62**, pp. 13–27 (2013).

40. De, S., Agarwal, A.K., Chaudhuri, S., and Sen, S., *Modeling and Simulation of Turbulent Combustion*, Springer (2018).

41. Fox, R.O. and Varma, A., *Computational Models for Turbulent Reacting Flows*, Cambridge Univ. Press (2003).

Biographies

Mohammad Safarzadeh is a PhD student at Tarbiat Modares University, Iran, under the supervision of Professor Ghassem Heidarinejad and Dr. Hadi Pasdarshahri. He graduated in Mechanical Engineering from Shiraz University, Iran, in 2012 and obtained his MS degree from the same university in 2015. He is currently carrying out research on numerical simulation of fire and combustion.

Ghassem Heidarinejad is Professor of Mechanical Engineering at Tarbiat Modares University, Iran. He received his PhD degree from Massachusetts Institute of Technology. His research interests include numerical simulation of turbulent-combustion flows, hybrid cooling system and green buildings.

Hadi Pasdarshahri is Assistant Professor of Mechanical Engineering at Tarbiat Modares University, Iran, from where he obtained his PhD degree. His research interests include experimental and numerical study of domestic and industrial energy systems, energy optimization in buildings, and computational fluid dynamic.